

Bromoform in the tropical boundary layer of the Maritime Continent during OP3

J. A. Pyle^{1,2}, M. J. Ashfold¹, N. R. P. Harris¹, A. D. Robinson¹, N. J. Warwick^{1,2}, G. D. Carver^{1,2}, B. Gostlow¹, L. M. O'Brien¹, A. J. Manning³, S. M. Phang⁴, S. E. Yong⁵, K. P. Leong⁵, E. H. Ung⁶, and S. Ong⁶

¹Department of Chemistry, University of Cambridge, Lensfield Road, Cambridge, CB2 1EW, UK

²National Centre for Atmospheric Science, NCAS, UK

³Met Office, Exeter, UK

⁴Institute of Ocean and Earth Science, University of Malaya, 50603 Kuala Lumpur, Malaysia

⁵Malaysian Meteorological Department, Ketua Stesen GAW Lembah Danum, Jabatan Meteorologi Malaysia Cawangan Sabah, Lapangan Terbang Wakuba Tawau, Peti Surat 60109, 91011 Tawau, Sabah, Malaysia

⁶Global Satria Life Sciences Lab, TB 12188, Taman Megajaya Phase 3, 91000 Tawau, Sabah, Malaysia

Received: 29 April 2010 – Published in Atmos. Chem. Phys. Discuss.: 21 June 2010

Revised: 12 November 2010 – Accepted: 17 December 2010 – Published: 18 January 2011

Abstract. We report measurements of bromoform made by gas chromatography during the OP3 campaign in 2008. Measurements were made simultaneously for a few days at the World Meteorological Organization (WMO) Global Atmospheric Watch (GAW) site in the Danum Valley, a rainforest location in Sabah, Borneo, and at a nearby coastal site at Kunak. Background values at Kunak were higher than those measured in the rainforest (2–5 ppt compared with 1 ppt) and excursions away from the background were very much higher, reaching 10 s of ppt. Measurements of C₂Cl₄, an industrial tracer, showed no significant difference in background at the two sites. Modelling using two different models can reproduce a number of the observed features. The data are consistent with a strong, local coastal source of bromoform in eastern Sabah and can be used to infer the strength of the source of bromoform in South East Asia. However, they provide only a very weak constraint on global emissions. The global model results highlight the difficulty for short-lived species of extrapolating limited duration, local measurements to a global source.

1 Introduction and background

Two major field campaigns of the multi-national OP3 (Oxidant and particle photochemical processes above a south-east Asian tropical rainforest) project took place during 2008 in

Sabah, Malaysia, on the island of Borneo. The OP3 project aims were wide-ranging, focussed on the better understanding of the interactions between natural forests, atmospheric composition and the Earth's climate system. A wide range of measurements explored biogenic emissions and their contribution to the oxidizing capacity of the troposphere. For example, measurements of isoprene fluxes from the forest and from palm oil plantations were an important component of OP3 and first results describing the potential implications of land use change for atmospheric isoprene concentrations and for oxidising capacity have been presented by Hewitt et al. (2009). The detailed objectives of OP3, and some preliminary results, are described by Hewitt et al. (2010).

An important sub-focus of OP3 was the investigation of the role of halogen species. Several groups made measurements of halocarbons (see Table 1 in Hewitt et al., 2010) and there was also a supporting modelling effort. There are a number of pressing reasons to study halocarbons in the tropics. Firstly, recent measurements at the Cape Verde Observatory have indicated that halogen species play an important role in controlling tropical oxidizing capacity (Read et al., 2008). The source of the halogen radicals is not well understood so further measurements of potential source gases are required; measurements of both radical and source gases were an OP3 objective. Secondly, there is some evidence that the rainforest might be a direct source of some halocarbons. A number of studies have looked at possible biogenic sources of halocarbons (principally CH₃Cl, but including other chloro- and bromocarbons), with the sources including plants, leaf litter, wood-rotting fungi and insects (Harper, 1985; Hoekstra et al., 1998; Yokouchi et al., 2002; Gebhardt



Correspondence to: J. A. Pyle
(john.pyle@atm.ch.cam.ac.uk)

et al., 2008; Mead et al., 2008; Saito et al., 2008). Thirdly, there is increasing interest in the role of natural, short-lived halogen species, which could potentially be lifted rapidly to the low stratosphere in deep convection where they could play a role in stratospheric ozone destruction (see, for example, Law et al., 2007). The Maritime Continent is likely the most important tropical location for this rapid transport (see, e.g., Levine et al., 2008), and characterising the background concentrations of these short-lived compounds, and their variability, in that region is an important research objective.

Halocarbons have both natural and anthropogenic sources. The anthropogenic sources are largely well understood and production of the major gases is controlled under the Montreal Protocol and its amendments (see, e.g., WMO, 2007). Many of the shorter-lived compounds are believed to be emitted naturally and the tropical oceans represent a major source. For example, bromoform (CHBr_3) is the major natural contributor of organic bromine to the atmosphere (Penkett et al., 1985; Carpenter and Liss, 2000; Quack and Wallace, 2003); it is predominantly oceanic in origin, with tropical macroalgae constituting an important source (Gschwend et al., 1985). An open ocean source, related to phytoplankton, has also been identified (Tokarczyk and Moore, 1994).

The short-lived biogenic halocarbons have been measured in very variable concentrations in a number of different locations, emphasizing the importance of localized emissions of these compounds, which show both temporal and spatial variability. For example, CHBr_3 , with a tropical lifetime with respect to photolysis and reaction with hydroxyl (OH) radicals of two to three weeks (Warwick et al., 2006), exhibits large spatial variability. Class and Ballschmiter (1988), Quack et al. (2004) and Carpenter et al. (2007) report mixing ratios of CHBr_3 over the eastern tropical Atlantic Ocean, ranging from a minimum of about 0.2 ppt to maxima around 25 ppt. O'Brien et al. (2009) deployed a version of the gas chromatograph used in this study at the Cape Verde Observatory in June 2007. During a measurement period of about 10 days they reported mixing ratios of bromoform with a background of about 4 ppt but with episodes of much higher mixing ratios to greater than 40 ppt. Shallow coastal areas seem to be particularly important for emissions of oceanic halocarbons. Yokouchi et al. (2005) observed a maximum of 40 ppt of CHBr_3 at the coasts of San Cristobal and Christmas Islands in the tropical Pacific Ocean. Highest measured concentrations of polybromomethanes coincided with the on-shore sea breeze, across the coastal zone. A number of studies show CHBr_3 and CH_2Br_2 to be well correlated in coastal locations, suggesting a common source for these compounds (for example see Quack et al., 2007; Yokouchi et al., 2005; O'Brien et al., 2009).

Measurements of short-lived species inevitably display large variability. Determining the global significance of these measurements is a difficult task, as is deciding the optimum measurement strategy. As a first step towards that strategy,

it is clear that more measurements of the short-lived halocarbons, including bromoform, are required to allow better understanding of their sources and to characterise variability. This was among the OP3 objectives. In this paper we focus on a comparison between rainforest and coastal measurements of two halocarbons by gas chromatography to investigate differences between the coast and inland. We report data taken during June 2008 when for a few days two of the Cambridge μ -Dirac instruments, as previously deployed in Cape Verde, made simultaneous measurements in Borneo from the GAW site at Bukit Atur (4.98°N , 117.85°E) and at Kunak (4.70°N , 118.24°E), a coastal site about 50 km from Bukit Atur which overlooks Darvel Bay, the largest bay in Eastern Sabah. The μ -Dirac gas chromatograph with electron capture detector (GC-ECD) (Gostlow et al., 2010; O'Brien et al., 2009) can measure a range of halocarbons and was designed in-house to make long term, autonomous measurements. Here two identical instruments were deployed. Demonstrating good agreement between these two is a prerequisite for future large scale deployments of more instruments. We focus here on measurements of the predominantly biogenic species, bromoform. Our scientific aim is to explore any differences between the bromoform measurements at the two sites and to see how different large scale numerical modelling tools can be used in the interpretation of these local measurements. We also consider to what extent these data can be used to constrain current global emission estimates. For purposes of comparison, measurements of an anthropogenic species, C_2Cl_4 , are also presented here.

The next section introduces the tools used in this study. First we present a brief description of μ -Dirac and then we outline p-TOMCAT and NAME, two different models used here. Section 3 presents the data while Sect. 4 aims to interpret the data using the models. Section 5 discusses uncertainties in our approach. An outlook for future work is presented in Sect. 6.

2 Experimental tools

2.1 The μ -Dirac gas chromatograph

μ -Dirac is an inexpensive, purpose-built gas chromatograph (GC) with electron capture detector (ECD), which has been designed to make long-term in-situ measurements of a small number of halocarbons (Gostlow et al., 2010; O'Brien et al., 2009). Its relatively low cost and ease of operation mean that multiple instruments can be deployed straightforwardly at a number of surface sites, thereby providing a valuable constraint on variability and emission estimates. μ -Dirac was originally designed for flights on long duration balloons and so is lightweight and able to operate autonomously. It is well suited for long periods of unattended operation. Earlier versions have been deployed on balloons, at ground-based sites and on aircraft (Robinson et al., 2000, 2005; Ross et

al., 2004). The GC has a modular design with an adsorbent tube containing ~ 1 mg each of Carboxen 1016 and 1001, which removes the target halocarbons from the air. A fixed volume of 20 scc is collected for each atmospheric sample, with a sampling time of approximately 1.5 min. The adsorbent is then flash heated and the sampled halocarbons are passed through a chromatographic column (Restek MXT 502.2, length 20 m, internal diameter 0.18 mm, film thickness 1 μ m) with temperature and flow programming capability. After temporal separation in the column the flow passes through the micro cell ECD (Agilent Technologies, model G2397-60510), which is extremely sensitive to halocarbons. The absolute calibration for most of the reported gases (including both the gases discussed here) is determined by reference to a NOAA-ESRL calibration standard (SX-3542 certified in December 2005), using an on-board standard gas cylinder (Restek Sulfinert® part no. 22113) filled directly with air from the NOAA-ESRL standard. Mixing ratios are reported as dry air mole fraction in ppt. Although the on-board cylinder was not compared with the NOAA ESRL standard at the end of the campaign we know any wall losses were small over this timescale due to the excellent agreement between our data and that from a GC-MS operated by University of East Anglia at Danum during the campaign (Gostlow et al., 2010). Our NOAA-ESRL standard was also measured by the UEA GC-MS during the campaign and a dry air mole fraction for bromoform of 8.1 ppt was determined compared to the NOAA certified value of 9 ppt.

Two instruments were taken to Borneo for OP3. Various modes of operation, and locations, were trialled. One instrument was always housed in an air-conditioned laboratory at the GAW site at Bukit Atur in the Danum Valley and collected data via a tube at 10 m on the tower. The second instrument sometimes made measurements side-by-side with the first instrument, including measurements at various heights up the 100 m GAW tower. It was sometimes deployed elsewhere, including overnight on the forest floor in an attempt to detect local rainforest sources and, for the case discussed here, at a fish-farm building a few metres from the shore of the large bay at Kunak. In either case, the run cycle was roughly 14 minutes, with a blank sample and a calibration standard being sampled on average after ten atmospheric samples (i.e. every 2 to 3 h). The instrument was cooled internally with Peltier coolers. The species that are measured include: CFC-11, CFC-113, CH_3CCl_3 , CCl_4 , CH_3I , $\text{CHCl}_2\text{Br}/\text{CH}_2\text{Br}_2$, C_2Cl_4 , and CHBr_3 . In this paper we report measurements of CHBr_3 and C_2Cl_4 , natural and anthropogenic species respectively, for a short period during June and July 2008. Gostlow et al. (2010) show a comparison of CHBr_3 measurements made side-by-side by μ -Dirac and UEA GC-MS at Danum Valley during the deployment in July 2010, demonstrating excellent agreement (see Fig. 11 of that paper). μ -Dirac measurements of a number of species from two sites in Sabah have continued since 2008. When the currently on-going analysis is completed these data will be

reported in the literature. Measurement characteristics have been presented in detail in Table 1 of O'Brien et al. (2009) and in Gostlow et al. (2010) so we do not repeat that here. Suffice to say that for CHBr_3 and C_2Cl_4 the overall uncertainties are $\pm 8\%$ and $\pm 4\%$ respectively (1σ values).

2.2 The models

We have used two different models, p-TOMCAT and NAME, to analyse the halocarbon data we collected during OP3. The basic formulation of the global chemistry and transport model p-TOMCAT is described in Cook et al. (2007) and Hamilton et al. (2008). Tracer transport is based on 6-hourly meteorological fields, including winds and temperatures, derived from European Centre for Medium-Range Weather Forecasts operational analyses for 2008. Here we use a high horizontal resolution ($0.5^\circ \times 0.5^\circ$) version of p-TOMCAT based on a previous, lower resolution version described by Warwick et al. (2006). This contains emissions of a set of short-lived bromocarbons, including bromoform. Bromoform tracers are “coloured” according to the geographical region of emission, allowing the contributions from different source regions to be calculated.

The degradation of the bromocarbons is determined using pre-calculated time-varying 3-D fields of OH and photolysis frequencies. The OH fields are prescribed hourly values taken from a previous p-TOMCAT integration and have been analysed and compared to other global OH distributions described in the literature following the method of Lawrence et al. (2001). They give a methane lifetime of 10.4 years and are within the range of other global model OH distributions, although OH concentrations are in the low end of the range in the tropical mid and upper troposphere. The photolysis frequencies are taken from an integration of the Cambridge 2-D model using cross section data summarised by Sander et al. (2003).

Bromoform emissions in this study are based on Scenarios 3 and 5 of Warwick et al. (2006). The approach in that study was to use remote free tropospheric bromoform measurements over the Pacific Ocean from the PEM Tropics campaign (Schauffler et al., 1999) to constrain open ocean emissions and determine an upper limit for the global coastal source. Scenarios 3 and 5 were presented as probable lower and upper bounds on the global source of bromoform. Emissions in Scenario 3 totalled 400 Gg CHBr_3/yr and are distributed in uniform bands over tropical and extra-tropical oceans, with tropical open oceans providing the major source of bromoform. Scenario 5 contained emissions of 595 Gg CHBr_3/yr , consisting of reduced open ocean emissions relative to Scenario 3 of 300 Gg CHBr_3/yr and 295 Gg CHBr_3/yr of tropical coastline emissions. However, as the simulations performed here are at a higher resolution than Warwick et al. (2006), we have generated an improved higher resolution, $0.5^\circ \times 0.5^\circ$, emission map, with a narrower coastal source region emitting the same global total as in Scenario 5.

Upgrading Scenario 5 from a resolution of $\sim 2.8^\circ \times 2.8^\circ$ (as in the original Warwick et al. (2006) study) to $0.5^\circ \times 0.5^\circ$ has two important impacts on the emission distribution. Firstly, coastal fluxes per unit area increase as the same global source is spread over a smaller, better defined coastal region. Secondly, the higher resolution land-sea mask used to define the coastal region in this study alters the geographical distribution of the coastal emissions. In the previous $2.8^\circ \times 2.8^\circ$ study, 57% of coastal emissions are located in the maritime SE Asia region (SEA, defined in Sect. 4). However, in this $0.5^\circ \times 0.5^\circ$ study, 70% of coastal emissions are located in the SEA region; the contribution of SEA emissions to the global total has increased with the change in resolution. As Scenario 3 does not contain coastal emissions, the per unit area fluxes and geographical distribution of emissions in this scenario are not significantly influenced by the change in resolution. Unless specifically stated otherwise, any subsequent reference to Scenarios 3 and 5 refers to the new high resolution version of these scenarios outlined here. As in Warwick et al. (2006), all the emissions are constant in time.

The Numerical Atmospheric dispersion Modelling Environment (NAME) is a Lagrangian particle dispersion model developed by the UK Met Office (see, e.g. Ryall and Maryon, 1998), which has been extensively used for analysis of long-term halocarbon data sets (e.g., Manning et al., 2003; Simmonds et al., 2006; Derwent et al., 2007). Abstract particles are moved through the model atmosphere by a combination of 0.5625° longitude by 0.375° latitude mean wind fields calculated by the UK Met Office Unified Model (Davies et al., 2005), and a random walk turbulence scheme. NAME can be run backwards in time, to see where the air measured at a particular site may have originated, and forwards to see where air from a particular emission source might go. Each of these capabilities have previously been used to investigate relationships between sources, transport and measurements of pollutants (e.g. Redington and Derwent, 2002; Webster et al., 2006; Witham and Manning, 2007). Both modes of operation are deployed here.

3 The data

We report data collected during June and July 2008. The two instruments were operated side-by-side at the GAW site on 16/17 June and one instrument was then transported the 53 km to Kunak, at the coast. Kunak is a small town with some industry, including a palm oil processing plant. We observed the bay at Kunak to be rich in macroalgae. We did not perform a systematic analysis at that time but did identify the brown, bromoform-producing *Sargassum* species (see, e.g., Class et al., 1986). A subsequent seaweed collection trip to Kunak in July 2008 resulted in the identification of brown seaweeds (*Sargassum*, *Dicyota*, *Hormophysa* and *Padina*), red seaweeds (*Amphiroa*, *Laurencia*, *Gracilaria*, *Hypnea*) and green seaweeds (*Caulerpa*, *Halimeda*, *Anady-*

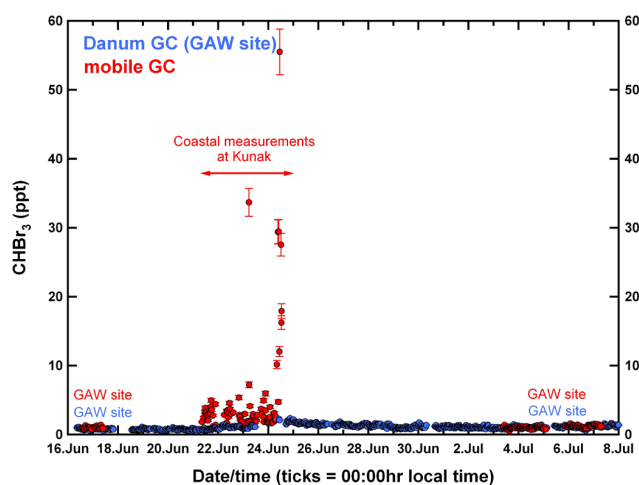


Fig. 1. Concentration of CHBr_3 (ppt) measured at Danum Valley and Kunak by the μ -Dirac GC. Blue symbols indicate measurements with the instrument deployed throughout at Danum Valley. Red symbols are concentrations measured by the instrument which was deployed at Kunak between 21 and 25 June, but otherwise was at Danum Valley.

omene, *Neomeris*). *Sargassum siliquosum* and *Sargassum myriocystum* were dominant. After four days of μ -Dirac measurements (21–24 June) the instrument was then returned to the GAW site in the Danum Valley and further side-by-side measurements were performed.

Figures 1 and 2 show our measurements of CHBr_3 and C_2Cl_4 . For both species, the two instruments made consistently similar measurements during side-by-side operation at Bukit Atur both before and after the Kunak deployment. It seems clear that any differences between Danum and Kunak should represent real atmospheric differences and not a change in instrument characteristics during the Kunak deployment (see below). The deployment thus represented an important successful test of the suitability of the instrument for long-term autonomous deployment. Demonstrating acceptable agreement between these instruments was an essential prerequisite, given our aim of placing at least five instruments in South East Asia for several years.

There are several prominent features in the bromoform data. First, the background values at Kunak of 2–5 ppt are considerably higher than those measured inland at the GAW site (~ 1 ppt) and more consistent with our Cape Verde measurements of May and June 2007 (O'Brien et al., 2009). Bromoform has a tropical lifetime of about 2 weeks, so such a large gradient across 50 km was surprising at first sight. In Sect. 4 we use the models to explore this question. Second, there are several occasions when extremely high mixing ratios, up to nearly 60 ppt, were measured. These were all cases with onshore winds and most likely represent the measurement of very local emissions.

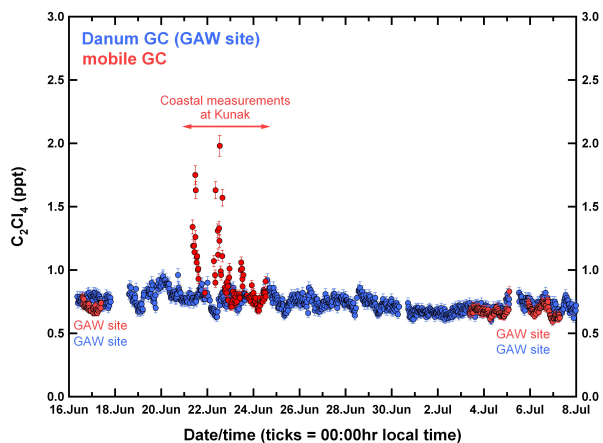


Fig. 2. Time series of measured concentrations of C_2Cl_4 . The colour scheme means the same as in Fig. 1.

C_2Cl_4 is a predominantly industrial compound used as a metal degreasing solvent and for dry cleaning. Unlike for $CHBr_3$, the baseline measurements of C_2Cl_4 at Kunak are comparable with the measurements at Danum Valley of 0.7–0.8 ppt. Like bromoform there are large excursions above the Kunak baseline of up to 2 ppt; however, these do not correlate with the bromoform peaks, suggesting that their origin is real and different to that of bromoform. It seems likely that they represent the influence of an industrial source, either locally at Kunak or from further down the coast towards Tawau (see Sect. 4).

To explore further the similarities and differences between the datasets, Fig. 3 plots the data as probability density functions (pdfs) from the various deployments, with results from the two instruments shown in different colours. Figure 3a, b confirm the instrumental consistency; the instruments in side-by-side operation show no important difference.

Figure 3c, d explores the differences between the Kunak and Danum measurements. For C_2Cl_4 , the baseline at Kunak is identical to that measured at Danum but the tail of higher values is evident. The behaviour for $CHBr_3$ is different. There is a broad spectrum of measured values at Kunak. There are only a few measurements with the low values consistent with Danum. Instead, the spread of measurements has a median of 2.7 ppt and quite a large standard deviation. To characterise this as a single “background” may be inappropriate. Instead we may be sampling a range of air parcels at Kunak from somewhat differing sources. Finally, the tail of very high values (>5 ppt) is also evident in Fig. 3d.

4 Modelling and data interpretation

In this section we will use two different models to explore a number of features of the bromoform data. We first use the NAME model to see whether we can explain the differ-

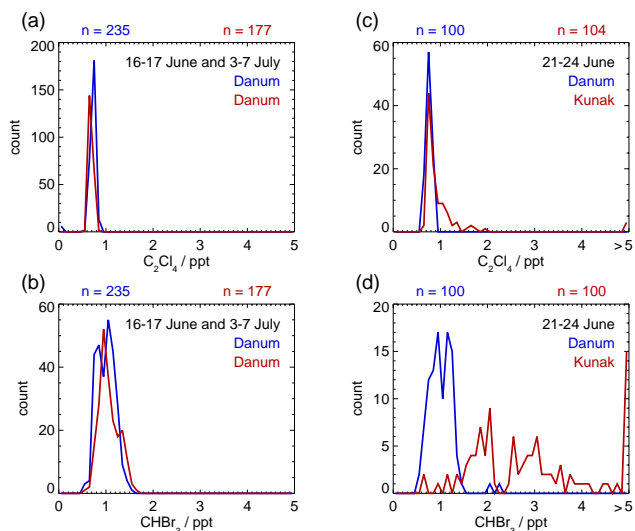


Fig. 3. Probability density functions (pdfs) for measurements made with μ -Dirac during OP3. One instrument remained at Bukit Atur, Danum Valley (blue). One instrument made measurements at Danum and at Kunak (red). (a) and (b) show, respectively, C_2Cl_4 and $CHBr_3$ measurements made while the instruments were co-located. (c) and (d) show measurements made while the instruments were at different sites. For each plot 0.1 ppt bins were used, and the number of measurements made by each instrument (n) is indicated above.

ent mixing ratios seen at Danum Valley and Kunak. Are the higher values measured at Kunak consistent with NAME calculations? In addition, can we use NAME to understand the very high values of bromoform occasionally seen at Kunak? NAME is also used to make an estimate of coastal emissions from the area upwind of our measurements. The global model, p-TOMCAT, is run at a lower effective resolution than NAME. It will be used to see to what extent the measurements, and the emissions inferred using NAME, can inform our understanding of regional and global emissions. In particular, are the coastal emissions determined using NAME consistent with the global model results using p-TOMCAT?

The NAME model was first run backwards in time to determine the dominant direction of flow to the measurement sites in Sabah. Figure 4 shows, for air parcels arriving at Kunak on 23 June, the footprint (time integrated particle density) in the lowest 100 m of the model atmosphere at any location during the previous 10 days. Warm colours show the highest fractions and indicate where the measured air parcel has been most sensitive to surface emissions. The meteorological situation during the Kunak deployment was stable and the pattern shown in Fig. 4 barely changes during the measurement period. The large scale flow is south-easterly with the air arriving at Kunak coming from the direction of northern Australia, across the Timor and east Java Seas within the Coral Triangle, before turning more southerly along the east coast of Borneo. These

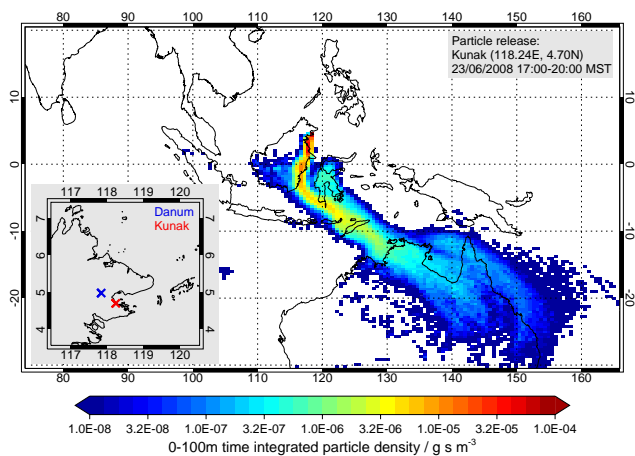


Fig. 4. Air mass history for Kunak. 30 000 particles, sharing 10.8 kg, were released from Kunak between 17:00 and 20:00 MST (UTC+8) on the 23 June 2008. They travelled backward in time for 10 days, with the position of particles in the lowest 100 m of the model atmosphere recorded every 15 minutes. At the end of the run, the particle mass below 100 m is integrated over the 10 day travel time. Warmer colours indicate a greater probability of a particle passing near the surface in a grid box. Inset: the location of the two measurements sites, 53 km apart; Danum (blue cross) and Kunak (red).

are potentially rich emission regions for halocarbons, with both the warm ocean and coastal areas possibly providing significant biological sources (as suggested, for example, by the ocean colour data available from <http://daac.gsfc.nasa.gov/giovanni/>). Seaweed farming is also important in these regions with the Coral Triangle producing 99% of the world's *Kappaphycus/Eucheuma*; bromoform and diodomethane are major halocarbons produced by *Eucheuma denticulatum* (Mtolera et al., 1996). These species of seaweed are farmed in Darvel Bay, where Kunak is located, and around Semporna, 50 km to the south east. These nearby farms cover 1500 ha with a production of 100 Tonnes DW per month (Phang, 2006). Both the natural populations of *Sargassum* at Kunak and the *Kappaphycus* and *Eucheuma* farms around Semporna could be sources of bromoform. In particular, with flow along the Borneo coast air parcels might have been expected to have picked up high concentrations of those bromocarbons emitted by macroalgae.

The flow shown in Fig. 4 offers a plausible explanation as to why high background concentrations of bromoform were measured at Kunak but cannot explain why the Kunak measurements are higher than those at Danum Valley. To explore this question, NAME was run forward in time. As running a dispersion model forwards in time with millions of particles is computationally expensive we chose to release particles only from those coastal regions that we know are likely to have influenced the measurement sites. By repeating the backwards calculations shown in Fig. 4 for each day

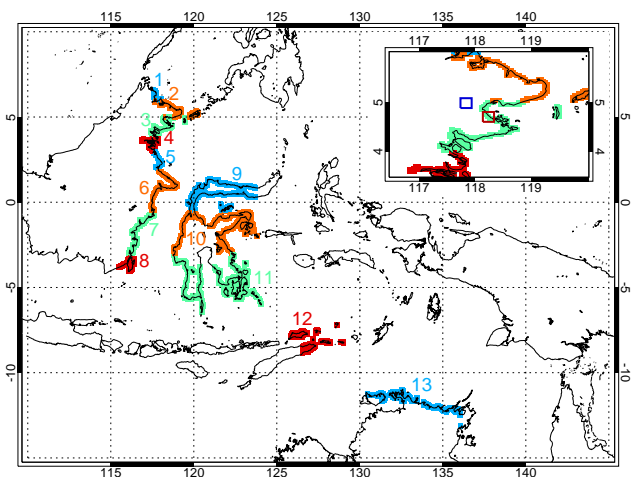


Fig. 5. Emission map for NAME forward run. To determine the emitting regions, the calculation presented in Fig. 4 was repeated for each day between 10 June and 31 July 2008 (approximately covering the period of our OP3 measurements). Grid boxes with a mean time integrated particle density greater than an arbitrary limit were selected. A 4 km resolution land-sea mask was then used to find coastlines within the selected grid boxes. These coastlines were then split in to 13 regions and populated with overlapping 0.1° emission squares. Inset: Danum (blue) and Kunak (red) are represented by 0.2° squares in the NAME model; Kunak contains emitting squares belonging to region 3.

of the OP3 measurements in June and July we know these to be the eastern coastal strip of Borneo, the coasts of Sulawesi and east Timor and the northernmost coastal strip of Australia, close to Darwin. Thirteen separate tracers are released from these regions as shown in Fig. 5. The mass on each particle has a specified e-folding lifetime of 15 days and is removed completely when the mass drops below 10% of the starting value. So, this experiment mimics the distribution of a coastally-emitted tracer, like bromoform (although bromoform also has an open ocean source). The emitting coastal boxes have dimensions $0.1^\circ \times 0.1^\circ$ and the emissions per unit area are constant. Note that the different regions in Fig. 5 do not have the same areas. Summing the individual tracers at any location gives the total tracer concentration there, assuming that all the tracer originates from our emitting regions, i.e., there is no “background” arising from longer-range transport. Time series of the total tracer distributions from this experiment for Kunak and Danum are shown in Fig. 6, where the vertical axis shows normalised concentrations (see the figure caption for an explanation of the conversion to mixing ratios). Results are for the lowest 100 m of squares of size 0.2° centred on the two locations. With our grid, Kunak directly experiences coastal emissions while Danum does not. The results in Fig. 6 show some similarities to Fig. 1. First, the concentrations at Danum (mean = 1.31 ppt) are usually (71% of the time) less than at Kunak (mean = 1.72 ppt), sometimes by a factor

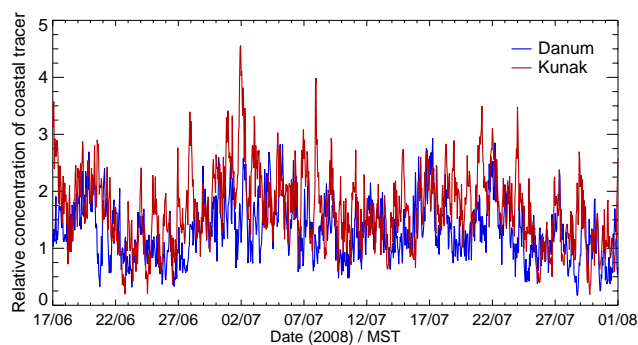


Fig. 6. Time series of the total tracer concentration for the lowest 100 m of 0.2° squares (see Fig. 5 inset) centred on Danum (blue) and Kunak (red). Each of the emitted particles is initialised in the model with an arbitrary mass, in this case of CHBr_3 -like tracer. We normalise the mean modelled particle concentration at Danum to the mean of our CHBr_3 measurements at Danum (1.31 ppt). The same scaling factor is applied to the modelled particle concentration at Kunak and the vertical axis then gives absolute mixing ratios in ppt. Finally, we scale the mass emitted on each particle to obtain our emission rate of 1.3 Gg CHBr_3/yr from the upwind coastlines.

of two or more, although this depends on the resolution of the output grid (see Sect. 5). Secondly the model for Kunak shows more high concentration excursions, as observed, and has a slightly higher variability (s.d. = 0.66 ppt) than Danum (s.d. = 0.51 ppt).

Figure 7 shows the contributions of the individual regional tracers to the total tracer concentrations at Kunak and Danum and affords further insight into their respective behaviours. It is clear that most of the difference between the two measurement sites arises from coastal emissions around and just to the south of Kunak (i.e., regions 3 and 4). The tracer concentration provided by region 3 is, on average, almost twice as large at Kunak as at Danum. The prevailing southerly winds during this period advect much of the tracer emitted from region 3 northward, reducing the impact upon Danum. These winds also ensure that Danum is marginally more influenced than Kunak by emissions from region 4 directly to the south. As we note above, 29% of the time the NAME model predicts higher total tracer concentrations at Danum than at Kunak. During our four days of measurements we never saw this feature but a much longer time series of data which we have collected since OP3, with measurements at Danum and Tawau, a coastal site just a little to the south of Kunak, does sometimes show this. It appears that the higher measurements at Kunak in late June 2008 are in part a result of the particular meteorological situation then. Finally, tracer emissions from regions far from northern Borneo have only a small impact on the total concentrations at Danum (or Kunak) and only make a very modest contribution to variability.

The pdfs for the modelled concentrations at Danum (blue) and Kunak (red) are shown in Fig. 8, for comparison with Fig. 3. The Kunak distribution is shifted to higher mixing ra-

tios, as observed, both distributions have a large spread (unlike the observations at Danum) and the model at Kunak fails to reproduce the tail of very high concentrations observed. We suspect they arise from small-scale, local emission “hot spots” which we have not attempted to model here.

For these NAME calculations, we have assumed that emissions per unit area are constant but in reality they are likely to vary due to natural (e.g., temperature, estuarine outflow impacting algal productivity, etc.) or anthropogenic (e.g., seaweed cultivation) factors. In this case, the weighting factors of the individual tracers to the total would not all be the same. If we do assume constant emissions, then it is possible to derive an emission estimate from the regions shown in Fig. 5. Scaling the NAME calculations to obtain a good agreement with the magnitude of the Danum observations (so that the vertical axis in Fig. 6 now gives absolute mixing ratios in ppt) implies an effective emission rate of 1.3 Gg CHBr_3/yr from the upwind coastlines (approximately the coastlines in regions 2–13 of Fig. 5). This value is an upper limit; in reality there will be some contribution from other regions.

We now use a second model, the global model p-TOMCAT, particularly to address the question of emission strengths. Both low resolution Scenarios 3 and 5 ($2.8^\circ \times 2.8^\circ$) in Warwick et al. (2006) were able to reproduce averaged free troposphere observations satisfactorily. However, Scenario 5 predicted high surface mixing ratios of bromoform of around 5 ppt over Borneo and other parts of SE Asia, arising from the high density of coastlines in this region (not seen in Scenario 3, see Fig. 2 of Warwick et al., 2006). When we perform a similar simulation with Scenario 5 emissions at the higher resolution of $0.5^\circ \times 0.5^\circ$, mixing ratios in South East Asia are even larger (~ 10 ppt) due to increased per unit area coastal fluxes in this region (see Sect. 2.2). These values are much higher than we observed in Borneo in 2008, as shown in Fig. 1. Although we have not repeated this calculation for the same model year (1996) as considered by Warwick et al. (2006), we anticipate that these higher surface mixing ratios in the $0.5^\circ \times 0.5^\circ$ simulation will also influence the signal seen in the free troposphere, probably leading to a less satisfactory comparison with the PEM tropics measurements than in the previous $2.8^\circ \times 2.8^\circ$ simulation.

Because of the overestimation of the surface measurements, we have performed additional calculations to attempt to refine the emission estimates. Since the emissions derived from our NAME calculations only consider the region to the south east of Borneo, we have only tried to change the p-TOMCAT emissions in the South-East Asia maritime region (10°N to 20°S , 90°E to 160°E , hereafter called SEA); elsewhere the emissions from Scenarios 3 and 5 are adopted in independent $0.5^\circ \times 0.5^\circ$ simulations. So, three separate ‘coloured’ bromoform tracers follow the emission contributions from (i) SEA coastlines, (ii) from SEA open ocean and (iii) from the rest of the world (RoW), where emission magnitudes are unchanged from the Warwick et al. (2006) study.

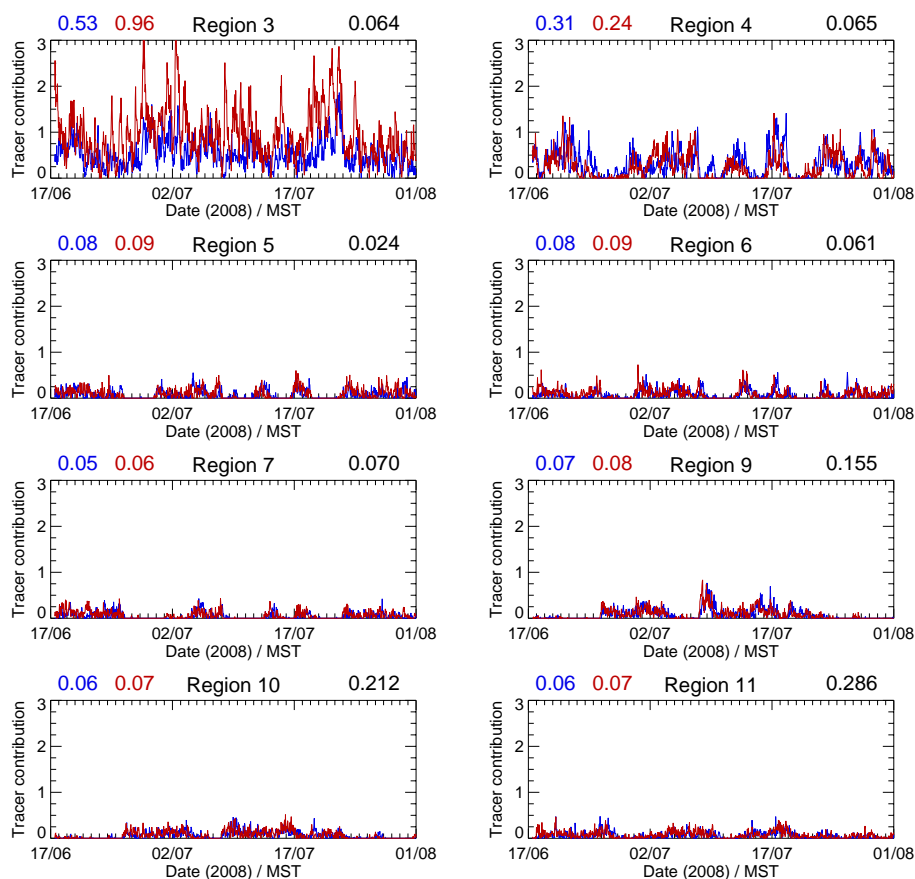


Fig. 7. Time series of regional tracer concentration for the lowest 100 m of 0.2° squares (see Fig. 5 inset) centred on Danum (blue) and Kunak (red). To the top left of each plot is the mean regional tracer contribution to Danum (blue) and Kunak (red). To the top right is the regional rate of emission (in Gg CHBr_3/yr). Due to their small impact we do not show the contributions from regions 1, 2, 8, 11 and 12. In total, the 5 excluded regions emit 0.3 Gg CHBr_3/yr ($\sim 25\%$ of the mass emitted from all regions combined) and supply $\sim 5\%$ of the total tracer concentration at both sites.

Table 1. Emission magnitudes required to provide matches between p-TOMCAT modelled bromoform and measurements of bromoform at the Danum Valley site in northern Borneo. Different geographical distributions of emissions within the SEA region require different emission magnitudes to reproduce the data. The fourth scenario (Scenario 5 RoW + SEA coastlines and open ocean, totalling 382 Gg CHBr_3/yr) is discussed further in the text as the “best fit”.

Emission Scenario	NAME Shaded Region (Gg/yr)	SEA Region (Gg/yr)	Rest of World (Gg/yr)	Global Total (Gg/yr)
SEA coastlines only	3.5	26	0	26
Scenario 5 RoW + SEA coastlines	2.8	21	352	373
Scenario 5 RoW + SEA open ocean	2.3	50	352	402
Scenario 5 RoW + SEA coastlines and open ocean	2.6	30	352	382
Scenario 3 RoW + SEA coastlines and open ocean	2.6	30	355	385

We find that the signal at Danum Valley from RoW emissions in Scenarios 3 and 5 is virtually identical and we cannot use our data to distinguish between the two scenarios outside of SEA. Modelled bromoform at Danum Valley from RoW emissions is less than a quarter of that observed; a regional

source is clearly required. Since it is likely that coastal emissions do make up an important fraction of the global bromoform source (e.g. Quack and Wallace, 2003), our subsequent analysis is based on Scenario 5 (but using Scenario 3 makes little difference).

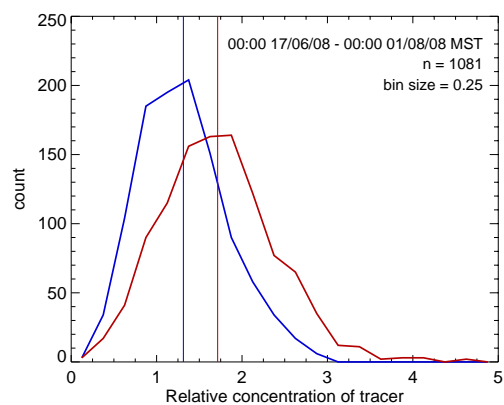


Fig. 8. Probability density functions (pdfs) for the NAME modelled concentrations at Danum (blue) and Kunak (red). 0.25 ppt bins were used, and the number of model time-steps from which the pdfs are calculated (1081) is indicated. Mean modelled concentrations are indicated by the solid vertical lines.

If we assume that bromoform is only emitted from coastlines in the SEA region (i.e. there is no background contribution from the rest of the world), then a source of 3.5 Gg CHBr₃/yr (in the following abbreviated to Gg/yr) from coastlines in the shaded NAME region in Fig. 4 is required to match the observations, about a factor three higher than inferred using NAME. Assuming spatially uniform coastline emissions across maritime South-East Asia, this scales to a total source of 26 Gg/yr from the whole SEA region, almost a factor of 10 less than in Scenario 5 (242 Gg/yr) and about half that in Scenario 3 (45 Gg/yr). The differences are in part a reflection of the additional constraint imposed here by the surface measurements, compared with just the free tropospheric measurements considered by Warwick et al. (2006). When RoW emissions are included they contribute to the bromoform background at Danum Valley; the total source required from the SEA coastline region and shaded NAME coastline region is reduced to 21 Gg/yr and 2.8 Gg/yr respectively. If instead a spatially uniform SEA open ocean source provides the additional bromoform required over the RoW background, then emissions of 50 Gg/yr (SEA region) and 2.3 Gg/yr (shaded NAME region) are required. When SEA sources from both coast and open ocean are included in addition to RoW emissions, a best fit of 30 Gg/yr (SEA region, distributed approximately evenly between coast and open ocean, based on a best model fit to observed magnitude and variability) and 2.6 Gg/yr (shaded NAME region) is found. The small differences arise from the balance between coastal and open ocean influence during this particular period. These results are summarised in Table 1. We can therefore conclude that our Danum Valley data are consistent with a range of emission magnitudes for the SEA region of 21 to 50 Gg/yr, with a best fit of 30 Gg/yr, depending on the assumed geographical distribution of the emissions.

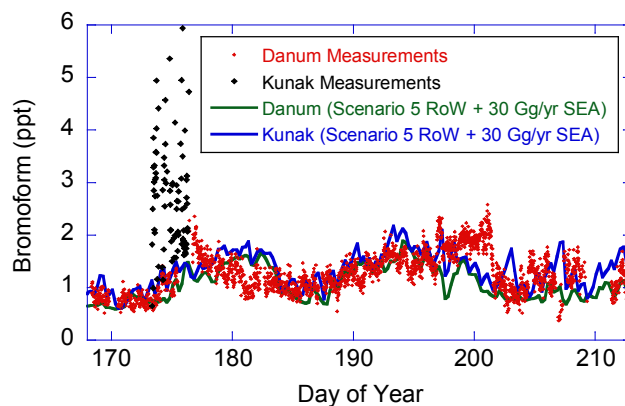


Fig. 9. A comparison of observed and modelled surface bromoform mixing ratios for Danum Valley and Kunak. Modelled mixing ratios are calculated using p-TOMCAT, with rest of world emissions as Scenario 5, Warwick et al. (2006) and SEA emissions scaled to 30 Gg CHBr₃/yr (16 Gg CHBr₃/yr from SEA open ocean and 14 Gg CHBr₃/yr from SEA coastlines). Global emissions in this scenario total 382 Gg CHBr₃/yr.

As the RoW bromoform tracer only contributes a small fraction to mixing ratios at Danum Valley, our measurements are relatively insensitive to the emission magnitude and distribution used outside of the SEA region. Therefore we cannot use our data alone to constrain global emissions of bromoform. However, we have considered the impact of updating previous global emission estimates by incorporating our new data for the SEA region. If our “best fit” emission estimate of 30 Gg/yr for the SEA region is combined with Scenario 3 RoW emissions, the total bromoform source in Scenario 3 decreases slightly from 400 Gg/yr in Warwick et al. (2006) to 385 Gg/yr. If it is combined with Scenario 5 RoW emissions, then the new total for Scenario 5 decreases substantially from 595 Gg/yr to 382 Gg/yr. Note that both these new scenarios are still consistent with remote tropical free tropospheric bromoform measurements of ~1 ppt observed in aircraft observations (Schaufler et al., 1999).

Figure 9 shows the June 2008 surface bromoform mixing ratios modelled using p-TOMCAT at Danum and Kunak for our “best fit” scenario (Scenario 5 RoW plus SEA coastlines and open ocean). With these emissions, the model is able to capture well the background mixing ratios at the inland measurement site at Danum. The model also captures a (small) concentration gradient between the coast and inland, consistent qualitatively with the differences in bromoform measured at our two sites (shown more clearly in Fig. 10). Similar to the NAME calculations, the gradient varies with the meteorological situation and sometimes we find no gradient or even a reverse gradient between Danum and Kunak. At the horizontal resolution of about 60 km, the model is, however, still unable to reproduce the large daytime peaks observed at Kunak and does not capture the magnitude of the differences between Danum and Kunak. The modelled “background” at

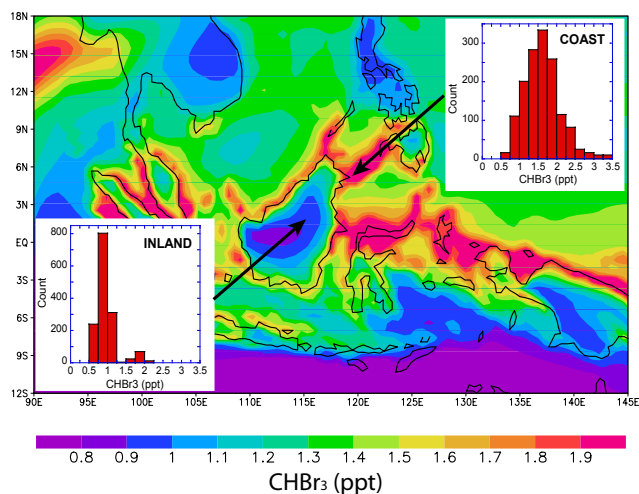


Fig. 10. Surface monthly mean June bromoform mixing ratios modelled by p-TOMCAT for the same scenario as in Fig. 9. The insets show the distribution of modelled mixing ratios through the month for an inland and coastal site.

Kunak is somewhat lower than observed, consistent with the coastal emissions at this resolution still being spread over too large an area.

5 Discussion

Warwick et al. (2006) and O'Brien et al. (2009) have both commented on the difficulty of using local, highly variable measurements of short-lived species to derive global emissions. These difficulties are compounded when the models used to assess or infer the emissions themselves contain inherent approximations and uncertainties. Thus, there could be problems in deriving emissions associated with a model's spatial and temporal averaging or due to inadequacies in the representation of physical processes. In this section we consider to what extent these issues could impact our aims of understanding the differences in the measurements at the two sites, including the higher background and peak concentrations observed at the coast, and in improving emissions estimates.

In Sect. 2, we mentioned the impact of changing the spatial resolution of the coastal emissions. On a coarse grid, such as used by Warwick et al. (2006), coastal emissions are smeared over a large spatial extent. When the same global emission magnitude was interpolated onto the $0.5^\circ \times 0.5^\circ$ grid, the emissions per unit area increased and, in this case, led to higher than observed average surface concentrations around the island of Borneo (see Sect. 4, above).

We tested further the impact of resolution by carrying out a model simulation with the best performing emission scenario (Scenario 5 RoW + 30 Gg/yr SEA) at a horizontal resolution of $1^\circ \times 1^\circ$ as well as $0.5^\circ \times 0.5^\circ$. Only very small differ-

ences were obtained between the $1^\circ \times 1^\circ$ and $0.5^\circ \times 0.5^\circ$ simulations of the Danum Valley grid box. The largest monthly mean differences occurred in coastal gridboxes and were still generally less than 0.2 ppt. However, as coastal emissions are believed to peak within 2 km of the shoreline (Quack and Wallace, 2003), a $0.5^\circ \times 0.5^\circ$ simulation, corresponding to approximately 60×60 km in the tropics, will still include considerable smearing of coastal emissions which will hamper comparisons with coastal measurements and possibly influence our estimate of total emissions in the SEA region. It is clearly not reasonable to expect the model to capture features associated with very local emissions (perhaps short time-scale, perhaps associated with a small seaweed bed) given that the model spreads its emissions uniformly across a large grid box and has a temporal resolution of several hours. Modelling at even higher resolution could potentially capture the impact of local emissions more faithfully, but deriving an emission data base at these resolutions would be a correspondingly difficult exercise.

Representing the emissions faithfully is not the only resolution-dependent issue for chemical transport models. Thus, at a horizontal resolution of about 60 km it is not expected that the sometimes sharp measured gradients between our measurement sites, situated 53 km apart, can be captured exactly in p-TOMCAT calculations. However, it is interesting that some meteorologically-driven gradients between coast and inland can evidently be reproduced, seen most clearly in Fig. 10 where we compare locations which are a few grid points apart.

In a further analysis of model uncertainty, we have used NAME to assess the potential variability within the p-TOMCAT grid boxes. Results from the NAME runs were sampled at $0.1^\circ \times 0.1^\circ$ (giving 25 output points for each p-TOMCAT grid box). Averaged over a two week period the concentration range within the p-TOMCAT grid box containing Danum Valley was about a factor of two; when smaller time intervals were considered the range became larger (for example, a factor 6 over an eight hour period). It is clearly not surprising that p-TOMCAT does not reproduce the same measurement statistics as the observations. Indeed, in reality the variability could be even greater than implied by the NAME calculations, which assumed that emissions per unit area were uniform over emitting regions. Local hot spots of very high emissions could contribute significantly to the observed variability. Inferring these emissions from measurements at a small number of sites would be a significantly under-constrained problem.

The intrinsic resolution in NAME is higher than in p-TOMCAT. NAME calculates forward trajectories and output can be on any chosen grid. Here the question is whether sufficient trajectory end points occur in the selected grid box. Clearly, the finer the resolution selected for the output grid, the more trajectories must be run to ensure significance. So, with the NAME output grid used here, the Kunak grid box directly experiences coastal emissions while Danum does not.

Higher resolution would likely degrade the statistics in Fig. 6 (fewer parcels per box) while a lower resolution would not allow us to distinguish between Danum and Kunak. Note that the resolution of the meteorological forcing fields is only $0.5625^\circ \times 0.375^\circ$ (although our experience is that low resolution winds on a high resolution grid can produce realistic structure). Recall also that trajectories were released on a grid of $0.1^\circ \times 0.1^\circ$, which again will influence the quality of any comparison with observations.

Another reason for the differences between NAME and p-TOMCAT could be their treatments of physical processes. The difference between NAME and p-TOMCAT emissions inferred from the shaded area in Fig. 4 is about a factor 3, with p-TOMCAT giving higher emissions. If the amounts of a tracer emitted from the shaded region which reach Danum are different in the two models, then different emissions would necessarily be inferred. So, for example, the model whose tracer, emitted into the boundary layer, mixes more quickly into the free troposphere would require higher emissions to match the surface observations. We have tried to assess this using a simple tracer release experiment in our two models. Tracers with lifetimes of about 15 days were released continuously for a month, with the emission region corresponding roughly to the shaded areas in Fig. 4. The last two weeks of the model runs were investigated. It was found that approximately 30% of the tracer in p-TOMCAT was below 2 km; the corresponding value for NAME was about 45%. The precise quantitative comparison is complicated by the different model structures, the somewhat different emission distributions and other small model differences. Nevertheless, it seems clear that one reason why p-TOMCAT infers a larger source strength relates to a stronger venting of boundary layer air into the free troposphere compared with NAME. Understanding these differences will be an important future objective.

6 Conclusions and further prospects

As part of the OP3 project, halocarbon measurements were made in 2008 at two sites in Sabah, Borneo, by gas chromatography using the μ -Dirac instrument. In this second field deployment of μ -Dirac the measurements confirmed the potential of the instrument for long-term observations at a range of sites for studies of halocarbon trends and for the determination of emissions. Observations with two identical instruments at Bukit Atur, Danum Valley, produced identical measurements of two different halocarbons, bromoform and C_2Cl_4 . When one instrument was then deployed at a nearby coastal site, higher concentrations of both species were measured. The bromoform background at the coast was higher than inland and the variability was also greater, with occasional peaks of many 10 s ppt. The background of C_2Cl_4 was the same at both sites but, again, the coastal measurements showed occasional very high values. In each case, the ex-

planation appears to lie with coastal sources. In the case of bromoform, these are likely to be related to macroalgae; for C_2Cl_4 industrial emissions from the populated coastal strip are the probable explanation.

Two different numerical models were used to aid data interpretation. The Lagrangian air parcel dispersion model, NAME, confirms that the air parcels during this period had crossed potentially rich oceanic and, especially, coastal regions prior to measurement in Sabah. NAME also shows that, despite a lifetime of about two weeks, substantial gradients between the coast and inland can be expected for bromoform, with the coastal measurement variability being dominated by local emissions. For the very short period of measurements undertaken, the coastal background was always higher than that measured inland. The modelling suggests that this need not always be the case, a result confirmed by a longer measurement series not reported here. The chemical transport model, p-TOMCAT, is able to reproduce the magnitude of the bromoform measurements but only if the emission strengths within the SEA region used by Warwick et al. (2006) are reduced. Depending on whether emissions are assumed to be predominantly from SEA open ocean or coastlines, and assuming a spatially and temporally uniform distribution, our measurements are consistent with emission rates of between 21 and 50 Gg $CHBr_3$ /yr for the SEA region. These values are consistent with Scenario 3 (45 Gg $CHBr_3$ /yr for SEA), which does not contain a coastal source of bromoform, but significantly less than in Scenario 5 (242 Gg $CHBr_3$ /yr for SEA), Warwick et al. (2006). If we were to reduce emissions globally in Scenario 5 by the same factors by which we reduce the SEA emissions to reproduce the Danum data, we would obtain a new global emission magnitude of 170 Gg $CHBr_3$ /yr. Emissions of this strength significantly underestimate remote tropospheric observations of bromoform (Schauffler et al., 1999). So, we would reject such a global extrapolation of our Borneo data. It is nevertheless interesting that our new best estimate is considerably lower than we reported earlier based on our short period of measurements at the Cape Verde observatory in 2007 (O'Brien et al., 2009), which was based on a global extrapolation of measured bromocarbon ratios. The difference further serves to emphasise the difficulty with using local measurements of short-lived halocarbons to infer global emissions.

Any model derivation of emissions needs to recognise model uncertainty. In particular, neither model has the resolution to capture very small scale features of transport, for example, the local sea breeze. Treatment of the boundary layer, as discussed in Sect. 5, will influence the inferred emissions strengths. Furthermore, modelling of the boundary layer in areas of complex topography like the Danum Valley (see, e.g., Pearson et al., 2010; Pike et al., 2010) will affect the modelled bromoform time series there and will also introduce uncertainty into our analysis. The calculations reported here are at a higher effective spatial resolution than many previous chemical transport studies; nevertheless, one focus

of future work needs to be the drive towards even higher resolution.

Tropical latitudes are clearly important for bromine emissions; given its short lifetime, reducing emission uncertainty further calls for bromoform measurements at a range of longitudes around the tropics. Furthermore, source estimates based on short local data records will also be subject to considerable uncertainty. We are addressing this latter issue by extending the deployment of μ -Dirac instruments in time and space. We now have nearly two annual cycles of measurements from two sites in Borneo (Bukit Atur, as reported here, and a new coastal site at Tawau, 85 km from Bukit Atur). These measurements will continue and will soon be complemented by the further installation of μ -Dirac at several new measurement sites in South East Asia.

Acknowledgements. This work was supported by a NERC consortium grant to the OP3 team (NE/D004217/1 at Cambridge), by NCAS and by the European Commission through the SCOUT-O3 project (505390-GOCE-CF2004). Louise O'Brien and Matt Ashfold thank NERC for research studentships. Andrew Robinson acknowledges NERC for their support through small grant project NE/D008085/1. Neil Harris is now supported by a NERC Advanced Research Fellowship (NE/GO/4655/1). We thank David Oram and Graham Mills from UEA for assistance with our calibration.

This is paper number 516 of the Royal Society's South East Asian Rainforest Research Programme.

Edited by: R. MacKenzie

References

- Carpenter, L. J. and Liss, P. S.: On temperate sources of bromoform and other reactive bromine gases, *J. Geophys. Res.*, 105(D12), 20539–20547, 2000.
- Carpenter, L., Wevill, D. J., Hopkins, J. R., Dunk, R. M., Jones, C. E., Hornsby, K. E., and McQuaid, J. B.: Bromoform in tropical Atlantic air from 25° N to 25° S, *Geophys. Res. Lett.*, 34, L11810, doi:10.1029/2007/GL029893, 2007.
- Class, T. H. and Ballschmiter, K.: Chemistry of organic traces in air: sources and distribution of bromo- and bromochloromethanes in marine air and surfacewater of the Atlantic Ocean, *J. Atmos. Chem.*, 6, 35–46, 1988.
- Class, T. H., Kohnle, R., and Ballschmiter, K.: Chemistry of organic traces in air VII: bromo- and bromochloromethanes in air over the Atlantic Ocean, *Chemosphere*, 15(4), 429–436, 1986.
- Cook, P. A., Savage, N. H., Turquety, S., Carver, G. D., O'Connor, F. M., Heckel, A., Stewart, D., Whalley, L. K., Parker, A. E., Schlager, H., Singh, H. B., Avery, M. A., Sachse, G. W., Brune, W., Richter, A., Burrows, J. P., Purvis, R., Lewis, A. C., Reeves, C. E., Monks, P. S., Levine, J. G., and Pyle, J. A.: Forest fire plumes over the North Atlantic: p-TOMCAT model simulations with aircraft and satellite measurements from the ITOP/ICARTT campaign, *J. Geophys. Res.*, 112, D10S43, doi:10.1029/2006JD007563, 2007.
- Davies, T., Cullen, M. J. P., Malcolm, A. J., Mawson, M. H., Staniforth, A., White, A. A., and Wood, N.: A new dynamical core for the Met Office's global and regional modelling of the atmosphere, *Q. J. Roy. Meteorol. Soc.*, 131, 1759–1782, 2005.
- Derwent, R. G., Simmonds, P. G., Grealley, B. R., O'Doherty, S., McCulloch, A., Manning, A. J., Reimann, S., Folini, D., and Vollmer, M. K.: The phase-in and phase-out of European emissions of HCFC-141b and HCFC-142b under the Montreal Protocol: Evidence from observations at Mace Head, Ireland and Jungfraujoch, Switzerland from 1994–2004, *Atmos. Environ.*, 41, 757–767, 2007.
- Gebhardt, S., Colomb, A., Hofmann, R., Williams, J., and Lelieveld, J.: Halogenated organic species over the tropical South American rainforest, *Atmos. Chem. Phys.*, 8, 3185–3197, doi:10.5194/acp-8-3185-2008, 2008.
- Gostlow, B., Robinson, A. D., Harris, N. R. P., O'Brien, L. M., Oram, D. E., Mills, G. P., Newton, H. M., Yong, S. E., and Pyle, J. A.: μ -Dirac: An autonomous instrument for halocarbon measurements, *Atmos. Meas. Tech.*, 3, 507–521, doi:10.5194/amt-3-507-2010, 2010.
- Gschwend, P. M., Macfarlane, J. K., and Newman, K. A.: Volatile Halogenated Organic-Compounds Released To Seawater From Temperate Marine Macroalgae, *Science*, 227, 1033–1035, 1985.
- Hamilton, J. F., Allen, G., Watson, N. M., Lee, J. D., Saxton, J. E., Lewis, A. C., Vaughan, G., Bower, K. N., Flynn, M. J., Crosier, J., Carver, G. D., Harris, N. R. P., Parker, R. J., Remedios, J. J., and Richards, N. A. D.: Observations of an atmospheric chemical equator and its implications for the tropical warm pool region, *J. Geophys. Res.*, 113, D20313, doi:10.1029/2008JD009940, 2008.
- Harper, D. B.: Halomethane From Halide Ion - A Highly Efficient Fungal Conversion Of Environmental Significance, *Nature*, 315, 55–57, 1985.
- Hoekstra, E. J., De Leer, E. W. B., and Brinkman, U. A. T.: Natural formation of chloroform and brominated trihalomethanes in soil, *Environ. Sci. Technol.*, 32, 3724–3729, 1998.
- Hewitt, C. N., MacKenzie, A. R., Di Carlo, P., Di Marco, C. F., Dorsey, J. R., Evans, M., Fowler, D., Gallagher, M. W., Hopkins, J. R., Jones, C. E., Langford, B., Lee, J. D., Lewis, A. C., Lim, S. F., McQuaid, J., Misztal, P., Moller, S. J., Monks, P. S., Nemitz, E., Oram, D. E., Owen, S. M., Phillips, G. J., Pugh, T. A. M., Pyle, J. A., Reeves, C. E., Ryder, J., Siong, J., Skiba, U., and Stewart, D. J.: Nitrogen management is essential to prevent tropical oil palm plantations from causing ground-level ozone pollution, *Proc. Natl. Acad. Sci.*, 106, 18447–18451, 2009.
- Hewitt, C. N., Lee, J. D., MacKenzie, A. R., Barkley, M. P., Carslaw, N., Carver, G. D., Chappell, N. A., Coe, H., Collier, C., Commane, R., Davies, F., Davison, B., DiCarlo, P., Di Marco, C. F., Dorsey, J. R., Edwards, P. M., Evans, M. J., Fowler, D., Furneaux, K. L., Gallagher, M., Guenther, A., Heard, D. E., Helfter, C., Hopkins, J., Ingham, T., Irwin, M., Jones, C., Karunaharan, A., Langford, B., Lewis, A. C., Lim, S. F., MacDonald, S. M., Mahajan, A. S., Malpass, S., McFiggans, G., Mills, G., Misztal, P., Moller, S., Monks, P. S., Nemitz, E., Nicolas-Perea, V., Oetjen, H., Oram, D. E., Palmer, P. I., Phillips, G. J., Pike, R., Plane, J. M. C., Pugh, T., Pyle, J. A., Reeves, C. E., Robinson, N. H., Stewart, D., Stone, D., Whalley, L. K., and Yin, X.: Overview: oxidant and particle photochemical processes above a south-east Asian tropical rainforest (the

- OP3 project): introduction, rationale, location characteristics and tools, *Atmos. Chem. Phys.*, 10, 169–199, doi:10.5194/acp-10-169-2010, 2010.
- Law, K. S., Sturges, W. T., Blake, D. R., Blake, N. J., Burkholder, J. B., Butler, J. H., Cox, R. A., Haynes, P. H., Ko, M. K. W., Kreher, K., Mari, C., Pfeilsticker, K., Plane, J. M. C., Salawitch, R. J., Schiller, C., Sinnhuber, B.-M., von Glasow, R., Warwick, N. J., Wuebbles, D. J., and Yvon-Lewis, S. A.: Halogenated very short-lived substances, Chapter 2 in Scientific Assessment of Ozone Depletion: 2006, Global Ozone Research and Monitoring Project, Rep. No. 50, World Meteorological Organization, Geneva, Switzerland, 2007.
- Lawrence, M. G., Jockel, P., and von Kuhlmann, R.: What does the global mean OH concentration tell us? *Atmos. Chem. Phys.*, 1, 37–40, doi:10.5194/acp-1-37-2001, 2001.
- Levine, J. G., Braesicke, P., Harris, N. R. P., and Pyle, J. A.: Seasonal and inter-annual variations in troposphere-to-stratosphere transport from the tropical tropopause layer, *Atmos. Chem. Phys.*, 8, 3689–3703, doi:10.5194/acp-8-3689-2008, 2008.
- Manning, A. J., Ryall, D. B., Derwent, R. G., Simmonds, P. G., and O'Doherty, S.: Estimating European emissions of ozone-depleting and greenhouse gases using observations and a modeling back-attribution technique, *J. Geophys. Res.*, 108, 4405, doi:10.1029/2002JD002312, 2003.
- Mead, M. I., Khan, M. A. H., Nickless, G., Grealley, B. R., Tainton, D., Pitman, T., and Shallcross, D. E.: Leaf cutter ants: a possible missing source of biogenic halocarbons, *Environ. Chem.*, 5, 5–10, 2008.
- Mtolera, M. S. P., Collen, J., Pedersen, M., Ekdahl, A., Abrahamsson, K., and Sesemi, A. K.: Stress-induced production of volatile halogenated organic compounds in *Eucheuma denticulatum* (Rhodophyta) caused by elevated pH and high light intensities, *Eur. J. Phycol.*, 31, 89–95, 1996.
- O'Brien, L. M., Harris, N. R. P., Robinson, A. D., Gostlow, B., Warwick, N., Yang, X., and Pyle, J. A.: Bromocarbons in the tropical marine boundary layer at the Cape Verde Observatory – measurements and modelling, *Atmos. Chem. Phys.*, 9, 9083–9099, doi:10.5194/acp-9-9083-2009, 2009.
- Penkett, S. A., Jones, B. M. R., and Rycroft, M. J.: An interhemispheric comparison of the concentrations of bromine compounds in the atmosphere, *Nature*, 318, 550–553, 1985.
- Phang, S. M.: Seaweed resources in Malaysia: Current status and future prospects, *Aqua. Ecosyst. Health Manage.*, 9(2), 185–202, 2006.
- Pike, R. C., Lee, J. D., Young, P. J., Carver, G. D., Yang, X., Warwick, N., Moller, S., Miszta, P., Langford, B., Stewart, D., Reeves, C. E., Hewitt, C. N., and Pyle, J. A.: NO_x and O₃ above a tropical rainforest: an analysis with a global and box model, *Atmos. Chem. Phys.*, 10, 10607–10620, doi:10.5194/acp-10-10607-2010, 2010.
- Pearson, G., Davies, F., and Collier, C.: Remote sensing of the tropical rain forest boundary layer using pulsed Doppler lidar, *Atmos. Chem. Phys.*, 10, 5891–5901, doi:10.5194/acp-10-5891-2010, 2010.
- Quack, B. and Wallace, D. W. R.: Air-sea flux of bromoform: Controls, rates and implications, *Global Biogeochem. Cy.*, 17(1), 1023, doi:10.1029/2002GB001890, 2003.
- Quack, B., Atlas, E., Petrick, G., Schauffler, S., and Wallace, D.: Oceanic bromoform sources for the tropical atmosphere, *Geophys. Res. Lett.*, 31, L23505, doi:10.1029/2004GL020597, 2004.
- Quack, B., Atlas, E., Petrick, G., and Wallace, D. W. R.: Bromoform and dibromomethane above the Mauritanian upwelling: Atmospheric distributions and oceanic emissions, *J. Geophys. Res.-Atmos.*, 112, D09312, doi:10.1029/2006JD007614, 2007.
- Read, K. A., Mahajan, A. S., Carpenter, L. J., Evans, M. J., Faria, B. V. E., Heard, D. E., Hopkins, J. R., Lee, J. D., Moller, S. J., Lewis, A. C., Mendes, L., McQuaid, J. B., Oetjen, H., Saiz-Lopez, A., Pilling, M. J., and Plane, J. M. C.: Extensive halogen-mediated ozone destruction over the tropical Atlantic Ocean, *Nature*, 453, 1232–1235, doi:10.1038/nature07035, 2008.
- Redington, A. L. and Derwent, R. G.: Calculation of sulphate and nitrate aerosol concentrations over Europe using a Lagrangian dispersion model, *Atmos. Environ.*, 36, 4425–4439, 2002.
- Robinson, A. D., McIntyre, J., Harris, N. R. P., Pyle, J. A., Simmonds, P. G., and Danis, F.: A lightweight balloon-borne gas chromatograph for in-situ measurements of atmospheric halocarbons, *Rev. Sci. Instr.*, 71, 4553–4560, 2000.
- Robinson, A. D., Millard, G. A., Danis, F., Guirlet, M., Harris, N. R. P., Lee, A. M., McIntyre, J. D., Pyle, J. A., Arvelius, J., Dagnesjo, S., Kirkwood, S., Nilsson, H., Toohey, D. W., Deshler, T., Goutail, F., Pommereau, J.-P., Elkins, J. W., Moore, F., Ray, E., Schmidt, U., Engel, A., and Müller, M.: Ozone loss derived from balloon-borne tracer measurements and the SLIMCAT CTM, *Atmos. Chem. Phys.*, 5, 1423–1436, doi:10.5194/acp-5-1423-2005, 2005.
- Ross, D. E. M., Pyle, J. A., Harris, N. R. P., McIntyre, J. D., Millard, G. A., Robinson, A. D., and Busen, R.: Investigation of Arctic O₃ depletion sampled over midlatitudes during the Egrett campaign of spring/summer 2000, *Atmos. Chem. Phys.*, 4, 1407–1417, doi:10.5194/acp-4-1407-2004, 2004.
- Ryall, D. B. and Maryon, R. H.: Validation of the UK Met. Office's NAME model against the ETEX dataset, *Atmos. Environ.*, 32, 4265–4276, 1998.
- Saito, T., Yokouchi, Y., Kosugi, Y., Tani, M., Philip, E., and Okuda, T.: Methyl chloride and isoprene emissions from tropical rainforest in Southeast Asia, *Geophys. Res. Lett.*, 35, L19812, doi:10.1029/2008GL035241, 2008.
- Sander, S. P., Finlayson-Pitts, B. J., Friedl, R. R., Golden, D. M., Huie, R. E., Kolb, C. E., Kurylo, M. J., Molina, M. J., Moortgat, G. K., Orkin, V. L. and Ravishankara, A. R.: Chemical kinetics and photochemical data for use in atmospheric studies, Evaluation 14, JPL Publ. 02-25, Jet Propul. Lab., Pasadena, CA, USA, 2003.
- Schauffler, S. M., Atlas, E. L., Blake, D. R., Flocke, F., Lueb, R. A., Lee-Taylor, J. M., Stroud, V., and Travnicek, W.: Distributions of brominated organic compounds in the troposphere and lower stratosphere, *J. Geophys. Res.*, 104(D17), 21513–21535, doi:10.1029/1999JD900197, 1999.
- Simmonds, P. G., Manning, A. J., Cunnold, D. M., McCulloch, A., O'Doherty, S., Derwent, R. G., Krummel, P. B., Fraser, P. J., Dunse, B., Porter, L. W., Wang, R. H. J., Grealley, B. R., Miller, B. R., Salameh, P., Weiss, R. F., and Prinn, R. G.: Global trends, seasonal cycles, and European emissions of dichloromethane, trichloroethene, and tetrachloroethene from the AGAGE observations at Mace Head, Ireland, and Cape Grim, Tasmania, *J. Geophys. Res.*, 111, D18304, doi:10.1029/2006JD007082, 2006.
- Tokarczyk, R. and Moore, R. M.: Production of volatile organohalogen by phytoplankton cultures, *Geophys. Res. Lett.*,

- 21(4), 285–288, 1994.
- Warwick, N. J., Pyle, J. A., Carver, G. D., Yang, X., Savage, N. H., O'Connor, F. M., and Cox, R. A.: Global modeling of biogenic bromocarbons. *J. Geophys. Res.*, 111, D24305, doi:10.1029/2006JD007264, 2006.
- Webster, H. N., Abel, S. J., Taylor, J. P., Thomson, D. J., Haywood, J. M., and Hort, M. C.: Dispersion Modelling Studies of the Buncefield Oil Depot Incident, Hadley Centre, technical note 69, 2006.
- Witham, C. and Manning, A.: Impacts of Russian biomass burning on UK air quality, *Atmos. Environ.*, 41, 8075–8090, 2007.
- World Meteorological Organisation (WMO): Scientific Assessment of Ozone Depletion 2006: Global ozone research and monitoring project, Rep. 50., World Meteorol. Org., Geneva, 2007.
- Yokouchi, Y., Ikeda, M., Inuzuka, Y., and Yukawa, T.: Strong emission of methyl chloride from tropical plants, *Nature*, 416, 163–165, 2002.
- Yokouchi, Y., Hasebe, F., Fujiwara, M., Takashima, H., Shiotani, M., Nishi, N., Kanaya, Y., Hashimoto, S., Fraser, P., Toom-Sauntry, D., Mukai, H., and Nojiri, Y.: Correlations and emission ratios among bromoform, dibromochloromethane, and dibromomethane in the atmosphere, *J. Geophys. Res.*, 110, D23309, doi:10.1029/2005JD006303, 2005.